Title

Enhancing Graphene Protective Coatings by Hydrogen-Induced Chemical Bond Formation

Journal

ACS Applied Nano Materials, 1(9)

ISSN

2574-0970

Authors

Kyhl, Line

Balog, Richard

Cassidy, Andrew

et al.

Publication Date

2018-09-28

DOI

10.1021/acsanm.8b00610

Peer reviewed

ACS APPLIED NANO MATERIALS

Article

Cite This: ACS Appl. Nano Mater. 2018, 1, 4509−4515

www.acsanm.org

Enhancing Graphene Protective Coatings by Hydrogen-Induced Chemical Bond Formation

Line Kyhl,[†,∥] Richard Balog,[‡] Andrew Cassidy,[‡] Jakob Jørgensen,[†,⊥] Antonija Grubisic-Čabo,[†,#] Lena Trotochaud,[§] Hendrik Bluhm,[§] and Liv Hornekær*[,†,‡]

[†]iNANO and [‡]Department of Physics and Astronomy, University of Aarhus, DK-8000 Aarhus C, Denmark

[§]Chemical Sciences Division, Lawrence Berkeley National Lab, Berkeley, California 94720, United States

ABSTRACT: Increased interactions at the graphene−metal interface are here demonstrated to yield an effective prevention of intercalation of foreign species below the graphene cover. Hereby, an engineering pathway for increasing the usability of graphene as a metal coating is demonstrated. Graphene on Ir(111) (Gr/Ir(111)) is used as a model system, as it has previously been well-established that an increased interaction and formation of chemical bonds at the graphene−Ir interface can be induced by hydrogen functionalization of the graphene from its top side. With X-ray photoelectron spectroscopy, it is shown that hydrogen-induced increased interactions at the Gr/Ir(111) interface effectively prevents intercalation of CO in the millibar range. The scheme leads to protection against at least 10 times higher pressure and 70 times higher fluences of CO, compared to the protection offered by pristine Gr/Ir(111).

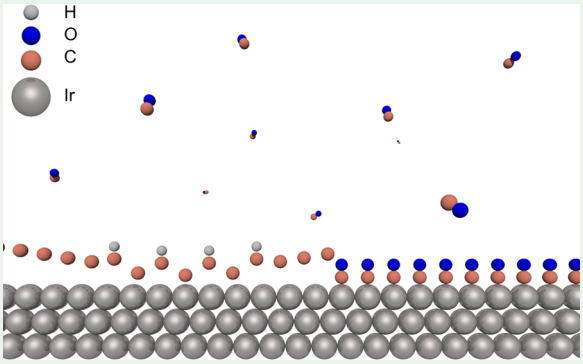

KEYWORDS: *graphene, coatings, intercalation, interface, XPS*

INTRODUCTION

Graphene is a two-dimensional (2D) semimetal consisting of pure sp^2 hybridized C atoms in a hexagonal lattice conformation.[1] The graphene basal plane is inert and impenetrable to most species.[2] For this reason, graphene has been suggested to perform well as a physical barrier between metal surfaces and oxidizing species, thus being suitable for corrosion protection.[3−6] Graphene possesses additional properties that may be desirable for coating applications, for example, high flexibility,[7] visual transparency,[8] and the ultimate thinness of one atomic layer.

Demonstrations of graphene performing as an anticorrosion coating for a range of metals, like Cu,[4,9−11] Pt,[12−14] Ni,[4,15,16] Ru,[17] Fe,[18] and stainless steel 304,[19] exposed to various corrosive environments, such as air, seawater, O_2, and CO, have been reported. Several studies, however, show that wrinkles,[20−22] grain boundaries,[6,21] and atomic and structural defects[22−24] lead to failure of the graphene coating. These imperfections in the graphene layer can promote reactions with oxidizing species and facilitate intercalation below the graphene cover. Once intercalation occurs, intercalants are likely to diffuse also toward areas covered by defect-free graphene sheets. The presence of graphene may, in such cases, be antiprotective, since graphene here acts as a source of electrons that stimulate galvanic corrosion processes on the metal surface.[25] Therefore, attempts to eliminate direct exposure of defective areas to reactive species have been explored. For example, a few-layer graphene coating makes a direct horizontal overlap between defects in the different layers unlikely, which in turn increases the diffusion length for intercalating species toward the metal surface. This makes few-layer graphene more efficient as a coating.[3,5,26] Alternatively, improvement of the coating by passivation of defects in graphene using Cu adatoms has also been demonstrated.[24]

It has previously been suggested that graphene−metal systems exhibiting a high interaction at their interface are less prone to intercalation, when compared to weakly interacting systems.[27] Here we investigate the effect of increasing the interaction in graphene−metal systems via chemical functionalization. The test system is graphene on an Ir(111) substrate. This system represents a weakly bound van der Waals system with an average binding energy of 55 meV/C atom.[28] Upon CO intercalation the binding energy drops to 22 meV/C atom. Hence, for intercalation to proceed, the energy gain from the newly formed Ir−CO interaction must exceed the energy cost associated with decoupling the graphene sheet. The condition can be met when a sufficient amount of CO covers the Ir(111) surface, which consequently determines a critical CO pressure for intercalation to occur.[28−30] This behavior indicates that by increasing the interaction between graphene and the Ir substrate it may be possible to prevent the intercalation process if sufficiently large interaction strength can be achieved.

Received: May 13, 2018
Accepted: August 23, 2018
Published: August 23, 2018

DOI: 10.1021/acsanm.8b00610
ACS Appl. Nano Mater. 2018, 1, 4509−4515

While the graphene sheet interacts weakly with Ir(111),[31,32] the interaction is modulated with a ∼25 Å periodicity due to a mismatch of ∼10% between the lattice constants of graphene and Ir(111).[33] See a sideview sketch of graphene on Ir(111) in Figure 1a. The largest interaction is found in areas of the moiré

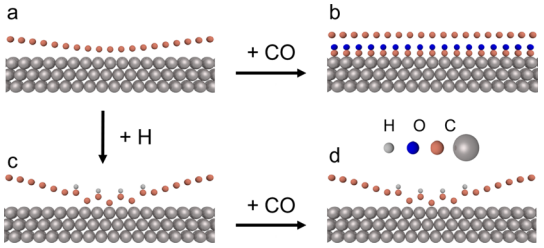

Figure 1. Sketch of (a) graphene on Ir(111), (b) CO intercalated graphene on Ir(111), (c) hydrogenated graphene on Ir(111), and (d) hydrogenated graphene on Ir(111) after CO exposure (not intercalated).

unit cell called the hexagonal close-packed (HCP) and face-centered cubic (FCC) areas, and the graphene−Ir distance is smallest here.[31] In earlier work we demonstrated that when H atoms chemisorb on top of C atoms in HCP and FCC areas, graphane-like structures[34,35] are formed. These single-sided hydrogenation structures represent clusters of fully sp^3 hybridized C atoms with alternating C−H and C−Ir bonds. See the sideview sketch of hydrogenated graphene on Ir(111) in Figure 1c. The functionalization with hydrogen therefore leads to an increased interaction strength in certain areas through covalent bond formation to the substrate. We also note that the most stable graphane-like clusters were found to be those comprising 7 to 12 C−H bonds, as revealed by scanning tunneling microscopy (STM) and density functional theory (DFT).[36]

RESULTS AND DISCUSSION

CO Intercalation. In the following, we demonstrate how H-functionalization of graphene and subsequent carbon−metal bond formation can be used to prevent the intercalation of CO molecules at the graphene−Ir interface, as sketched in Figure 1. We first measure the conditions that lead to intercalation of CO at the metal interface for Gr/Ir(111) and compare this to hydrogen-functionalized graphene (H-Gr/Ir(111)) at different stages of functionalization. We show that from a certain degree of H-functionalization the H-graphene coating eliminates intercalation under all tested conditions. X-ray photoelectron spectra (XPS) of the C 1s, Ir $4f_{7/2}$, and O 1s core levels were obtained on the Gr/Ir(111) sample before and after the CO test exposure and are presented in Figure 2a,b,c, respectively. Throughout this article the CO test exposure conditions, which lead to CO intercalation below a nonfunctionalized graphene coating, were 1 mbar CO with the sample kept at 473 K for 10 min. The temperature of 473 K was chosen, as it is below the desorption temperature of CO from Ir(111) (523 K, this work, not shown) but sufficiently high to enhance the intercalation rate. All XPS measurements related to CO exposure were performed after reduction of the CO pressure to 5×10^{-8} mbar, keeping the sample at 473 K. The C 1s core-level spectrum for the clean Gr/Ir(111) (Figure 2a, bottom panel) is fit using a single component, Cc, at 284.1 eV binding energy, representing sp^2 hybridized C atoms on the Ir(111) surface.[36−38] Upon exposure to CO, two new components, Ci

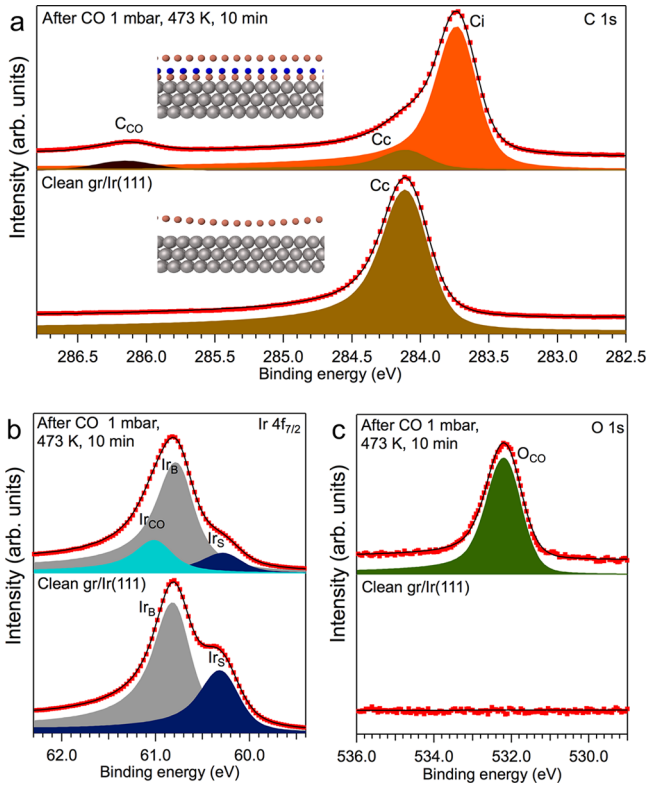

Figure 2. XPS core-level spectra of clean Gr/Ir(111) (bottom) and CO intercalated Gr/Ir(111), after exposure to 1 mbar CO, for 10 min, with the sample at 473 K (top). XPS measurements of the CO exposed sample were performed after reducing the CO pressure to 5×10^{-8} mbar, keeping the sample at 473 K. (a) C 1s ($h\nu$ = 490 eV). (bottom) Clean Gr/Ir(111), fit using the Cc component. (inset) A sideview sketch of nonintercalated Gr/Ir(111). (top) CO intercalated Gr/Ir(111), fit using the Cc, Ci, and C_{CO} components. (inset) A sideview sketch of CO intercalated Gr/Ir(111). (b) Ir $4f_{7/2}$ ($h\nu$ = 275 eV). (bottom) Clean Gr/Ir(111), fit using the Ir_B and Ir_S components. (top) CO intercalated Gr/Ir(111), fit using the Ir_B, Ir_S, and Ir_{CO} components. (c) O 1s ($h\nu$ = 735 eV). (bottom) Clean Gr/Ir(111), no oxygen species is present on the surface. (top) CO intercalated Gr/Ir(111), fit using the O_{CO} component.

and C_{CO}, are observed in the corresponding C 1s core-level spectrum, presented in Figure 2a, top panel. The Ci component, positioned at a binding energy of −0.37 eV relative to Cc, represents the intercalated graphene. An induced downshift in binding energy of more than 0.3 eV and a slight peak narrowing following CO intercalation are consistent with the findings by Grånäs et al.[28] The C_{CO} peak at 286.2 eV represents the CO adsorbed on the Ir(111) surface below the graphene. In Figure 2b the Ir $4f_{7/2}$ spectra for the sample before (bottom) and after (top) CO intercalation are shown. For the clean Gr/Ir(111) sample, the spectrum is fit using two components representing Ir bulk atoms (Ir_B) and Ir surface atoms (Ir_S), positioned at binding energies 60.79 and 60.28 eV, respectively. After CO intercalation, Figure 2b top, the Ir_S component has transformed into a new component, Ir_{CO}, at +0.23 eV relative to Ir_B. The Ir_{CO} component is assigned to CO adsorbed on Ir surface atoms, below the graphene, consistent with previous observations.[28]

In the O 1s spectra in Figure 2c, clearly oxygen is only present on the surface *after* the CO intercalation (top). The component denoted O_{CO} thus stems from oxygen in the CO molecules.

DOI: 10.1021/acsanm.8b00610
ACS Appl. Nano Mater. 2018, 1, 4509−4515

Prevention of CO Intercalation by H Functionalization. In Figure 3a–c, bottom panels, we show the C 1s, Ir

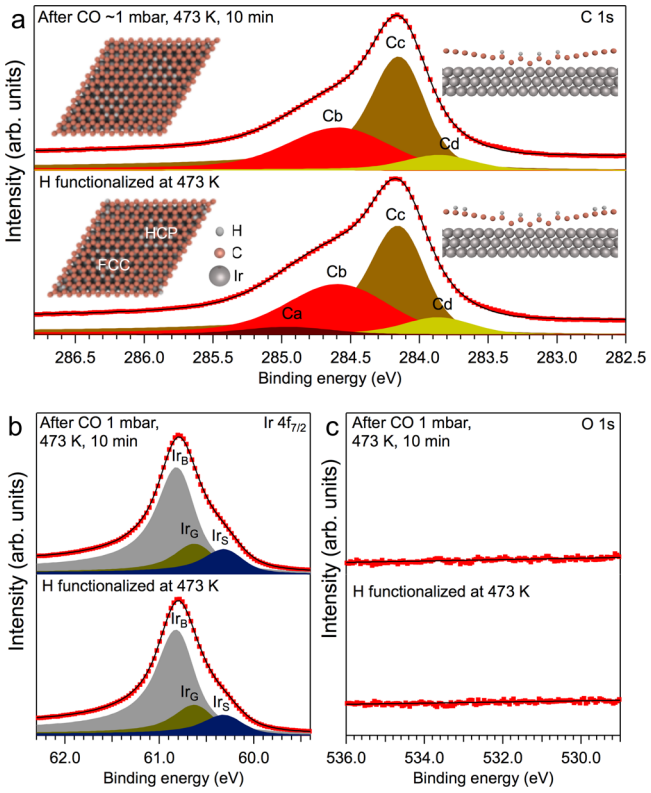

Figure 3. XPS core-level spectra of Gr/Ir(111) hydrogenated at 473 K (bottom) and the same sample after a subsequent exposure to 1 mbar CO for 10 min with the sample at 473 K (top). XPS measurements of the CO exposed sample were performed after reducing the CO pressure to 5×10^{-8} mbar, keeping the sample at 473 K. (a) C 1s ($h\nu$ = 490 eV), (bottom) H-Gr/Ir(111) fit using the Cc, Ca, Cb, and Cd components. (insets) Top- and side-view sketches of Gr/Ir(111) hydrogenated at 473 K. Hydrogen clusters form on FCC and HCP areas of the moiré unit cell, and dimer structures form outside these areas. (top) H-Gr/Ir(111) after CO exposure, fit using the Cc, Cb, and Cd components. No CO-related components are present. (insets) Top- and side-view sketches of the hydrogenated Gr/Ir(111) after the CO exposure, where only the most stable structures are present. (b) Ir $4f_{7/2}$ ($h\nu$ = 275 eV), (bottom) H-Gr/Ir(111) fit using the Ir_B, Ir_S, and Ir_G components. (top) H-Gr/Ir(111) after CO exposure, fit using Ir_B, Ir_S, and Ir_G components. No CO-related components are present. (c) O 1s ($h\nu$ = 735 eV), (bottom) H-Gr/Ir(111), no oxygen species are present. (top) H-Gr/Ir(111) after CO exposure, no CO or other oxygen-related species are present.

$4f_{7/2}$, and O 1s core-level spectra of H-functionalized graphene (H-Gr/Ir(111)) prepared by exposure of a 473 K Gr/Ir(111) sample to hot H atoms. The C 1s core-level spectrum of H-Gr/Ir(111) in Figure 3a, bottom, is fit using the Cc component, representing clean graphene, and three additional hydrogenation-related components: Ca, Cb, and Cd, positioned with binding energies of +0.81, + 0.44, and −0.27 eV relative to Cc, respectively.[37] The Ca component is assigned to H adsorption on Gr/Ir(111) away from HCP and FCC regions of the moiré pattern, where C–Ir bonds cannot be formed.[37] Such structures are most likely hydrogen dimers, similar to those observed on hydrogenated quasi-freestanding graphene, exemplified by graphite.[39] The Cb component is related to hydrogenation structures in HCP and FCC areas of the Gr/Ir(111) moiré, where the formation of graphane-like clusters is possible. The Cb component is thus directly linked to the formation of C–Ir bonds.[35,37,38] The Cd component is related to hydrogen vacancies in the graphane-like clusters and in general to sp^2 carbon atoms that are neighbors to sp^3 carbon.[37]

The Ir $4f_{7/2}$ core-level spectrum for the H-Gr/Ir(111) is shown in Figure 3b, bottom, and is fit with three components: The Ir_B, Ir_S, and a new component, Ir_G, positioned with a binding energy of +0.31 eV relative to the position of Ir_S. The Ir_G component corresponds to Ir surface atoms that make bonds with C atoms from the graphene, in the graphane-like clusters,[37] as sketched in the insets of Figure 3. No oxygen is present on the surface after hydrogenation, as evidenced by the featureless O 1s signal in Figure 3c bottom.

The H-functionalized graphene sample was further exposed to 1 mbar CO with a sample temperature of 473 K for 10 min. The corresponding C 1s spectra are presented in the top panels of Figure 3a–c. No indication of CO intercalation is observed in the spectra, as there are no intercalation-related components: No signal corresponding to C_{CO} or Ci is observed. Also, no oxygen-related species are present on the surface, as evidenced by the featureless O 1s signal in Figure 3c top.

Although the graphene overlayer protects the metal from exposure to CO at given conditions, a small decrease in the hydrogen coverage is observed as revealed by the absence of the Ca component but also by a minor decrease in the intensities of the Cb and Cd components. The decrease in intensity of the C–H-related components is accompanied by an increase of the Cc component indicating simple removal of hydrogen by the CO exposure without any etching of the graphene. From the disappearance of the Ca component it appears that CO efficiently reacts with adsorbed dimer structures. The small decrease in the Cb component points toward the removal of H from the periphery of large graphane-like structures.

An observed decrease of the Ir_G component in Figure 3b top concurs with the minor decrease in Cb, as both Ir_G and Cb are linked to graphane-like structures. Importantly, the absence of the Ir_{CO} component ascertains that no CO is adsorbed onto the Ir(111) surface after the exposure. The results, summarized in Figure 3, therefore show that hydrogenated graphene prevents the intercalation of CO at the graphene–metal interface under conditions that would normally lead to CO intercalation in the clean Gr/Ir(111) system.

To test the limits of the H-functionalized graphene, the sample was further exposed to a 10 times higher pressure of CO (10 mbar) with no observable signs of intercalation. The corresponding C 1s, Ir $4f_{7/2}$, and O 1s spectra are shown in Figure 4 after an exposure of 10 min, bottom panels, and after an additional 60 min exposure, top panels. The C 1s and Ir $4f_{7/2}$ core-level spectra show no features related to CO intercalation in either case. Importantly, after the initial decrease of H coverage under CO exposure evidenced by the data displayed in Figure 3, no further decrease in hydrogenation level was observed even for extended CO exposures, signifying the high stability of smaller graphane-like clusters and the hydrogenated graphene layer in general.

In summary, we find that hydrogenation of graphene/Ir(111) at 473 K prevents intercalation of CO at the graphene–Ir interface at CO pressure up to at least 10 times

DOI: 10.1021/acsanm.8b00610
ACS Appl. Nano Mater. 2018, 1, 4509–4515

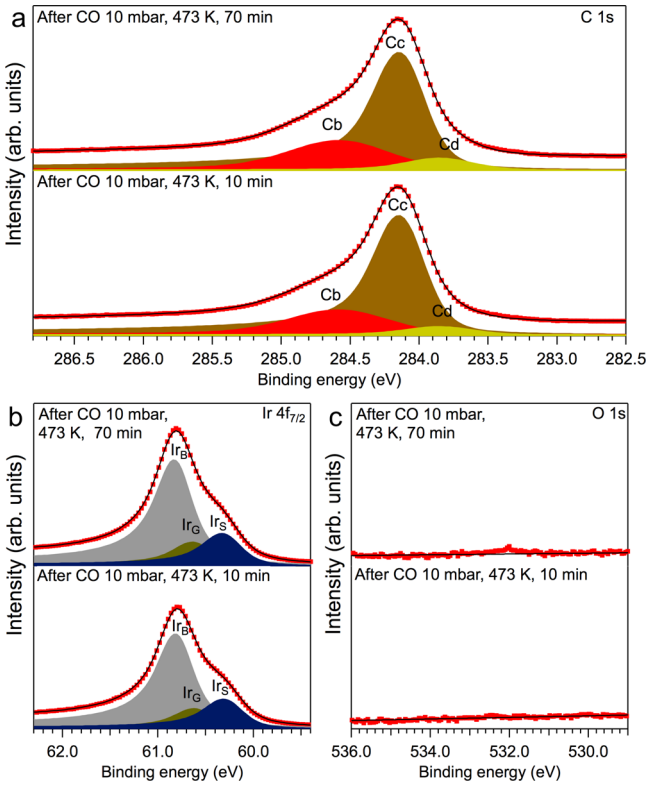

Figure 4. XPS core-level spectra of Gr/Ir(111), hydrogenated at 473 K, after a subsequent exposure to 10 mbar CO for 10 min (bottom) and for 70 min (top) while kept at 473 K. XPS measurements of the CO exposed sample were performed after reducing the CO pressure to 5×10^{-8} mbar, keeping the sample at 473 K. (a) C 1s ($h\nu$ = 490 eV), (bottom) H-Gr/Ir(111) after 10 min CO exposure, fit using the Cc, Cb, and Cd components. No CO-related components are present. (top) H-Gr/Ir(111) after 70 min of CO exposure, fit using the Cc, Cb, and Cd components. No CO-related components are present. (b) Ir $4f_{7/2}$ ($h\nu$ = 275 eV). (bottom) H-Gr/Ir(111) after 10 min of CO exposure, fit using the Ir_B, Ir_S, and Ir_G components. No CO-related components are present. (top) H-Gr/Ir(111) after 70 min of CO exposure, fit using the Ir_B, Ir_S, and Ir_G components. No CO-related components are present. (c) O 1s ($h\nu$ = 735 eV). (bottom) H-Gr/Ir(111) after 10 min of CO exposure, no oxygen species are present on the surface. (top) H-Gr/Ir(111) after 70 min of CO exposure; negligible oxygen is present on the surface.

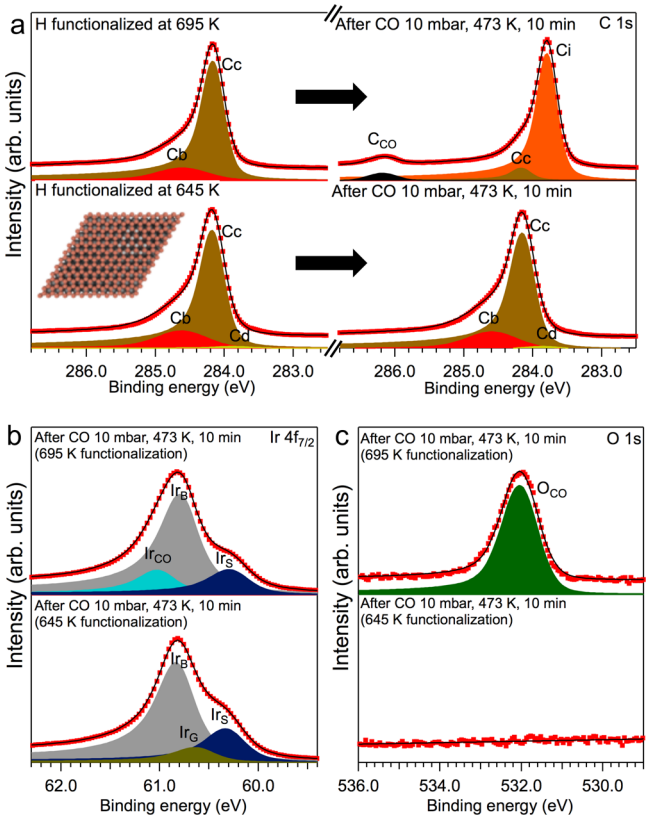

Figure 5. XPS core-level spectra of Gr/Ir(111) hydrogenated at 645 K (bottom left) and at 695 K (top left) and subsequently exposed to 10 mbar CO for 10 min while kept at 473 K (bottom and top right, respectively). XPS measurements of the CO-exposed samples were performed after reducing the CO pressure to 5×10^{-8} mbar, keeping the sample at 473 K. (a) C 1s ($h\nu$ = 490 eV). (bottom left) 645 K H-Gr/Ir(111) fit using the Cc, Cb, and Cd components. (inset) Sketches the situation where hydrogenation structures are only present on HCP areas of the moiré unit cell. (bottom right) 645 K H-Gr/Ir(111) after CO exposure, fit using the Cc, Cb, and Cd components. (top left) 695 K H-Gr/Ir(111) fit using the Cc and Cb components. (top right) 695 K H-Gr/Ir(111) after CO exposure, fit using the Cc, Ci, and C_{CO} components. (b) Ir $4f_{7/2}$ ($h\nu$ = 275 eV). (bottom) 645 K H-Gr/Ir(111) after CO exposure, fit using the Ir_B, Ir_S, and Ir_G components. (top) 695 K H-Gr/Ir(111) after CO exposure, fit using the Ir_B, Ir_S, and Ir_{CO} components. (c) O 1s ($h\nu$ = 735 eV). (bottom) 645 K H-Gr/Ir(111) after CO exposure, no oxygen species on the surface. (top) 695 K H-Gr/Ir(111) after CO exposure, fit using the O_{CO} component.

higher and at fluences at least 70 times higher than those leading to intercalation in the clean Gr/Ir(111) system.

Hydrogenation at Elevated Temperature. In the following we test the number density and distribution of C−Ir bonds necessary for the successful prevention of CO intercalation. Two different samples were prepared by hydrogenation at elevated sample temperatures of 645 and 695 K, respectively. The 645 K exposure delivers the most stable hydrogen clusters, namely, graphane-like structures in HCP areas only, as sketched at topview in the inset of Figure 5a. All other hydrogen configurations are not stable at this temperature, but the hydrogenation degree in the HCP areas is still high as demonstrated by STM measurements,[36] meaning that there is almost always one graphane-like cluster per moiré unit cell.[36] Thus, the 645 K exposure yields a homogeneous hydrogen coverage with localized clusters of graphane-like areas, each of which contains the required C−Ir bonds.

Exposing the Gr/Ir(111) to hot H atoms, with the sample at 695 K, yields an even lower hydrogen coverage, as some HCP areas are left without a hydrogen cluster, giving pure graphene in the entire moiré supercell.[36] Hence this sample with a lower hydrogen coverage also exhibits a substantially decreased number of C−Ir bonds.

In Figure 5a the C 1s core-level spectra of Gr/Ir(111) samples hydrogenated at 645 K, bottom left, and at 695 K, top left, are shown. The C 1s core-level spectra after the exposure of both samples to 10 mbar CO while kept at 473 K are shown in Figure 5a, bottom right and top right, respectively, for the 645 and 695 K case.

After the 10 mbar CO exposure, the 645 K H-Gr/Ir(111) remains unchanged, and no sign of any intercalation is observed as revealed by the absence of CO-related components in the C 1s (Figure 5a, bottom right) and Ir $4f_{7/2}$ (Figure 5b, bottom) core-level spectra but also by the

DOI: 10.1021/acsanm.8b00610
ACS Appl. Nano Mater. 2018, 1, 4509−4515

absence of oxygen-related features in the O 1s spectrum (Figure 5c, bottom).

On the contrary, the C 1s core-level spectrum for the 695 K H-Gr/Ir(111), after exposure to 10 mbar CO, resembles the spectrum of the CO intercalated graphene and consequently can be fit using the Cc, Ci, and C_{CO} components. Additionally, all sp^3-related carbon components are now transformed back to sp^2 type, meaning all hydrogen has been removed during the exposure.

The Ir $4f_{7/2}$ spectrum in Figure 5b, top, also reveals that CO has intercalated and hydrogen has desorbed from the graphene. This is evidenced by the presence of the Ir_{CO} component and the absence of the Ir_G component in the fit. The CO adsorption on the Ir(111) is additionally confirmed by the presence of the O_{CO} component in the O 1s spectra.

From Figure 5 it is thus evident that the Gr/Ir(111) hydrogenated at 645 K, that is, with a single graphane-like cluster in each moiré unit cell, prevents CO intercalation. The 695 K H-Gr/Ir(111) sample, however, does not protect, and the CO exposure leads to the removal of hydrogen and intercalation of CO at the graphene−Ir interface.

Previous experiments show that CO intercalates under graphene on Ir(111) at millibar pressures forming a $(3\sqrt{3} \times 3\sqrt{3})R30°$ structure.[28] STM measurements show a coverage of 0.7 ML, while DFT calculations predict binding energies of 1.59 eV per CO molecule. The CO intercalation results in a displacement of the graphene layer from a height of 3.51 to 6.42 Å and a decrease in graphene binding energy from 55 to 22 meV per carbon atom.[28] This results in a total binding energy for the system of CO-intercalated graphene on Ir(111) of 0.93 eV per graphene unit cell. This value can be compared to the binding energy of hydrogenated graphene on Ir(111). For surfaces hydrogenated at 645 K STM measurements show hydrogen coverages of 9%, indicating that 18% of C atoms are bound to either H or Ir atoms. The hydrogenated areas are placed in a regular array with a periodicity of ∼25 Å determined by the moiré structure. DFT calculations show that hydrogenated areas are pinned to the Ir(111) substrate at a distance of 2.2−2.4 Å, making the regularly functionalized structure incompatible with CO intercalation. Binding energies per H atom are of the order of 2.5 eV, resulting in a binding energy of 2.5 eV per graphene unit cell in the hydrogenated areas,[36] which makes this structure energetically more stable than the CO intercalation structure. In the case of hydrogenation at 695 K the hydrogen coverage falls below ∼8%, and missing hydrogen clusters in the hydrogenation array locally allow for CO intercalation. At such low hydrogen coverages the binding energy of CO dominates, and the hydrogenation structures are destabilized and desorb either thermally or via interaction with CO. The stability of the lower-temperature hydrogenation structures against reactions with CO is ascribed to the high binding energies (several eV) of these structures[36] and indicate that they may also be stable against more corrosive species.

CONCLUSIONS

Hydrogenation of graphene on an Ir substrate has been demonstrated to lead to the formation of strong bonds between the graphene and the metal substrate, which facilitate efficient prevention of intercalation of CO at the graphene−metal interface, thus increasing the protection of the graphene-based coating. The homogeneous distribution of interfacial bonding across a large area was observed to yield a protection against CO gas, up to at least 10 times higher pressure and 70 times higher fluence than that required to intercalate a pure graphene coating on Ir. Hydrogenated graphene on Ir(111) was used as a model system, but the results may well be transferable to other graphene-on-metal systems where interfacial C-metal bonds can form. The reported method may thus provide a means to enhance the properties of graphene-based materials as anticorrosion coating for metals.

EXPERIMENTAL SECTION

Gr/Ir(111) samples were prepared in a dedicated chamber with a base pressure of 5×10^{-10} mbar. A single-layer graphene was grown using ethylene gas by a combination of temperature-programmed growth (TPD) and chemical vapor deposition (CVD) as described elsewhere.[40,41] The Ir(111) crystals were cleaned by sputtering with high-energy Ar (5×10^{-6} mbar) ions at room temperature, followed by flash annealing to 1473 K. Afterward, oxygen (1×10^{-7} mbar, flash annealing to 1073 K, and cooling to 673 K) and hydrogen treatments (1×10^{-6} mbar, flash annealing to 1073 K, and cooling to 473 K) were performed to remove residual amorphous carbon and any remaining oxygen, respectively.

The CVD graphene growth parameters were 17 cycles of flash annealing to 1500 K in 5×10^{-7} mbar ethylene gas.

The pristine graphene samples were shipped to Berkeley, California, to perform the experiments at beamline 11.0.2, at the Advanced Light Source, Lawrence Berkeley National Laboratory. The experiments were performed under ultrahigh vacuum (UHV) conditions, with a base pressure of 1×10^{-9} mbar. The samples were annealed to 1100 K to desorb any contaminants, when reintroduced to UHV, prior to experiments. Cleanliness of the graphene samples was confirmed using XPS, after the introduction to, and annealing at, beamline 11.0.2.

CO intercalation experiments were performed at beamline 11.0.2 by backfilling the chamber to pressures in the millibar range, measured using a baratron gauge. The pressure was static in all cases. A high degree of beam damage on the graphene was observed when irradiating the sample at high CO pressure. The CO intercalation experiments were therefore performed using conventional XPS, when the pressure was reduced to 5×10^{-8} mbar after the CO exposures at higher pressures. The decrease of the CO pressure was not observed to affect the CO intercalation coverage over time. It can, however, not be excluded that an even higher coverage and/or other intercalation structures had been present during the high-pressure CO exposure.

The formation of C−Ir bonds at the graphene−Ir interface was obtained by exposing the Gr/Ir(111) to hot H atoms. The hot atoms were produced by running H_2 gas through a ∼2000 K W capillary, at a 4×10^{-7} mbar H_2 pressure for 10 min, keeping the sample in line of sight and ∼15 cm from the capillary outlet. Samples were kept at 473 K (Figures 3 and 4), 645 K (Figure 5, bottom panels), and 695 K (Figure 5, top panels) during hydrogenation. All hydrogenation was performed at beamline 11.0.2.

XPS C 1s, O 1s, and Ir $4f_{7/2}$ core-level data were fit using Doniach−Šunjić functions[42] convoluted with Gaussian functions. The backgrounds were fit using linear backgrounds (C 1s and O 1s) and Shirley-type backgrounds (Ir $4f_{7/2}$). The shapes and positions of the components used to fit C 1s and Ir $4f_{7/2}$ core-level spectra, representing H-Gr/Ir(111), were based on the work by Balog et al.[37] Shapes and positions of the components used to fit C 1s and Ir $4f_{7/2}$ spectra representing CO-intercalated Gr/Ir(111) were based on the work by Grånäs et al.[28]

AUTHOR INFORMATION

Corresponding Author

*E-mail: liv@phys.au.dk.

ORCID

Andrew Cassidy: 0000-0001-8352-8721

Antonija Grubisic-Čabo: 0000-0001-7683-0295

DOI: 10.1021/acsanm.8b00610
ACS Appl. Nano Mater. 2018, 1, 4509−4515

Lena Trotochaud: 0000-0002-8816-3781
Hendrik Bluhm: 0000-0001-9381-3155
Liv Hornekær: 0000-0003-0828-3642

Present Addresses

[‖]Unisense A/S, DK-8200 Skejby, Denmark.
[⊥]Bain & Company ApS, 1787 Copenhagen V, Denmark.
[#]School of Physics and Astronomy, Monash University, Victoria 3800, Australia.

Author Contributions

L.K., R.B., A.C., J.J., and L.H. designed the experiments. L.K., R.B., A.C., J.J., L.T., and H.B. performed the experiments. A.G.Č. prepared Gr/Ir(111) samples. L.K. analyzed the data and wrote the manuscript. All authors contributed to manuscript editing and discussions.

Funding

We acknowledge financial support from The Danish Council for Independent Research (Grant No. 0602-02566B and Grant No. 0602-02265B), Innovation Fund Denmark (NIAGRA), The European Research Council (CoG GRANN, Grant No. 648551), and VILLUM FONDEN via the Centre of Excellence for Dirac Materials (Grant No. 11744). Affiliation with the Center for Integrated Materials Research (iMAT) at Aarhus Univ. is gratefully acknowledged. H.B. acknowledges support by the Director, Office of Science, Office of Basic Energy Sciences, and by the Division of Chemical Sciences, Geosciences and Biosciences of the U.S. Department of Energy at Lawrence Berkeley National Laboratory (LBNL) under Contract No. DE-AC02-05CH11231. The Advanced Light Source is supported by the Director, Office of Science, Office of Basic Energy Sciences of the U.S. Department of Energy at LBNL under Contract No. DE-AC02-05CH11231.

Notes

The authors declare no competing financial interest.

■ ABBREVIATIONS

Gr/Ir(111), graphene on Ir(111)
H-Gr/Ir(111), hydrogenated graphene on Ir(111)
XPS, X-ray photoemission spectroscopy

■ REFERENCES

(1) Novoselov, K. S.; Geim, A. K.; Morozov, S. V.; Jiang, D.; Zhang, Y.; Dubonos, S. V.; Grigorieva, I. V.; Firsov, A. A. Electric Field Effect in Atomically Thin Carbon Films. *Science* **2004**, *306* (5696), 666−669.
(2) Achtyl, J. L.; Unocic, R. R.; Xu, L. J.; Cai, Y.; Raju, M.; Zhang, W. W.; Sacci, R. L.; Vlassiouk, I. V.; Fulvio, P. F.; Ganesh, P.; Wesolowski, D. J.; Dai, S.; van Duin, A. C. T.; Neurock, M.; Geiger, F. M. Aqueous Proton Transfer across Single-Layer Graphene. *Nat. Commun.* **2015**, *6*. DOI: 10.1038/ncomms7539
(3) Topsakal, M.; Sahin, H.; Ciraci, S., Graphene Coatings: An Efficient Protection from Oxidation. *Phys. Rev. B: Condens. Matter Mater. Phys.* **2012**, *85* (15). DOI: 10.1103/PhysRevB.85.155445
(4) Kirkland, N. T.; Schiller, T.; Medhekar, N.; Birbilis, N. Exploring Graphene as a Corrosion Protection Barrier. *Corros. Sci.* **2012**, *56*, 1−4.
(5) Prasai, D.; Tuberquia, J. C.; Harl, R. R.; Jennings, G. K.; Bolotin, K. I. Graphene: Corrosion-Inhibiting Coating. *ACS Nano* **2012**, *6* (2), 1102−1108.
(6) Kyhl, L.; Nielsen, S. F.; Cabo, A. G.; Cassidy, A.; Miwa, J. A.; Hornekaer, L. Graphene as an Anti-Corrosion Coating Layer. *Faraday Discuss.* **2015**, *180*, 495−509.
(7) Gomez-Navarro, C.; Burghard, M.; Kern, K. Elastic Properties of Chemically Derived Single Graphene Sheets. *Nano Lett.* **2008**, *8* (7), 2045−2049.
(8) Nair, R. R.; Blake, P.; Grigorenko, A. N.; Novoselov, K. S.; Booth, T. J.; Stauber, T.; Peres, N. M.; Geim, A. K. Fine Structure Constant Defines Visual Transparency of Graphene. *Science* **2008**, *320* (5881), 1308−1308.
(9) Chen, S. S.; Brown, L.; Levendorf, M.; Cai, W. W.; Ju, S. Y.; Edgeworth, J.; Li, X. S.; Magnuson, C. W.; Velamakanni, A.; Piner, R. D.; Kang, J. Y.; Park, J.; Ruoff, R. S. Oxidation Resistance of Graphene-Coated Cu and Cu/Ni Alloy. *ACS Nano* **2011**, *5* (2), 1321−1327.
(10) Huh, J. H.; Kim, S. H.; Chu, J. H.; Kim, S. Y.; Kim, J. H.; Kwon, S. Y. Enhancement of Seawater Corrosion Resistance in Copper Using Acetone-Derived Graphene Coating. *Nanoscale* **2014**, *6* (8), 4379−4386.
(11) Liang, Y. Q.; Yu, L. L.; Cui, Z. D.; Zhu, S. L.; Li, Z. Y.; Yang, X. J. Large-Scale Synthetic Graphene on Cu as Anti-Corrosion Coating by Chemical Vapor Deposition Approach. *Sci. Adv. Mater.* **2014**, *6* (3), 545−549.
(12) Mu, R. T.; Fu, Q.; Jin, L.; Yu, L.; Fang, G. Z.; Tan, D. L.; Bao, X. H. Visualizing Chemical Reactions Confined under Graphene. *Angew. Chem., Int. Ed.* **2012**, *51* (20), 4856−4859.
(13) Nilsson, L.; Andersen, M.; Balog, R.; Laegsgaard, E.; Hofmann, P.; Besenbacher, F.; Hammer, B.; Stensgaard, I.; Hornekaer, L. Graphene Coatings: Probing the Limits of the One Atom Thick Protection Layer. *ACS Nano* **2012**, *6* (11), 10258−10266.
(14) Nilsson, L.; Andersen, M.; Hammer, B.; Stensgaard, I.; Hornekaer, L. Breakdown of the Graphene Coating Effect under Sequential Exposure to O_2 and H_2S. *J. Phys. Chem. Lett.* **2013**, *4* (21), 3770−3774.
(15) Dedkov, Y. S.; Fonin, M.; Laubschat, C. A Possible Source of Spin-Polarized Electrons: The Inert Graphene/Ni(111) System. *Appl. Phys. Lett.* **2008**, *92* (5), 052506.
(16) Mogera, U.; Kurra, N.; Radhakrishnan, D.; Narayana, C.; Kulkarni, G. U. Low Cost, Rapid Synthesis of Graphene on Ni: An Efficient Barrier for Corrosion and Thermal Oxidation. *Carbon* **2014**, *78*, 384−391.
(17) Borca, B.; Calleja, F.; Hinarejos, J. J.; Vazquez de Parga, A. L.; Miranda, R. Reactivity of Periodically Rippled Graphene Grown on Ru(0001). *J. Phys.: Condens. Matter* **2009**, *21* (13), 134002.
(18) Dedkov, Y. S.; Fonin, M.; Rudiger, U.; Laubschat, C. Graphene-Protected Iron Layer on Ni(111). *Appl. Phys. Lett.* **2008**, *93* (2), 022509.
(19) John, R.; Ashokreddy, A.; Vijayan, C.; Pradeep, T. Single- and Few-Layer Graphene Growth on Stainless Steel Substrates by Direct Thermal Chemical Vapor Deposition. *Nanotechnology* **2011**, *22* (16), 165701.
(20) Zhang, Y. H.; Zhang, H. R.; Wang, B.; Chen, Z. Y.; Zhang, Y. Q.; Wang, B.; Sui, Y. P.; Zhu, B.; Tang, C. M.; Li, X. L.; Xie, X. M.; Yu, G. H.; Jin, Z.; Liu, X. Y. Role of Wrinkles in the Corrosion of Graphene Domain-Coated Cu Surfaces. *Appl. Phys. Lett.* **2014**, *104* (14), 143110.
(21) Vlaic, S.; Kimouche, A.; Coraux, J.; Santos, B.; Locatelli, A.; Rougemaille, N. Cobalt Intercalation at the Graphene/Iridium(111) Interface: Influence of Rotational Domains, Wrinkles, and Atomic Steps. *Appl. Phys. Lett.* **2014**, *104* (10), 101602.
(22) Petrovic, M.; Rakic, I. S.; Runte, S.; Busse, C.; Sadowski, J. T.; Lazic, P.; Pletikosic, I.; Pan, Z. H.; Milun, M.; Pervan, P.; Atodiresei, N.; Brako, R.; Sokcevic, D.; Valla, T.; Michely, T.; Kralj, M. The Mechanism of Caesium Intercalation of Graphene. *Nat. Commun.* **2013**, *4*, 2772.
(23) Wlasny, I.; Dabrowski, P.; Rogala, M.; Kowalczyk, P. J.; Pasternak, I.; Strupinski, W.; Baranowski, J. M.; Klusek, Z. Role of Graphene Defects in Corrosion of Graphene-Coated Cu(111) Surface. *Appl. Phys. Lett.* **2013**, *102* (11), 111601.
(24) Hsieh, Y. P.; Hofmann, M.; Chang, K. W.; Jhu, J. G.; Li, Y. Y.; Chen, K. Y.; Yang, C. C.; Chang, W. S.; Chen, L. C. Complete Corrosion Inhibition through Graphene Defect Passivation. *ACS Nano* **2014**, *8* (1), 443−448.

(25) Schriver, M.; Regan, W.; Gannett, W. J.; Zaniewski, A. M.; Crommie, M. F.; Zettl, A. Graphene as a Long-Term Metal Oxidation Barrier: Worse Than Nothing. *ACS Nano* **2013**, *7* (7), 5763−5768.
(26) Stoot, A. C.; Camilli, L.; Spiegelhauer, S.-A.; Yu, F.; Bøggild, P. Multilayer Graphene for Long-Term Corrosion Protection of Stainless Steel Bipolar Plates for Polymer Electrolyte Membrane Fuel Cell. *J. Power Sources* **2015**, *293*, 846−851.
(27) Weatherup, R. S.; D'Arsié, L.; Cabrero-Vilatela, A.; Caneva, S.; Blume, R.; Robertson, J.; Schloegl, R.; Hofmann, S. Long-Term Passivation of Strongly Interacting Metals with Single-Layer Graphene. *J. Am. Chem. Soc.* **2015**, *137* (45), 14358−14366.
(28) Grånäs, E.; Andersen, M.; Arman, M. A.; Gerber, T.; Hammer, B.; Schnadt, J.; Andersen, J. N.; Michely, T.; Knudsen, J. CO Intercalation of Graphene on Ir (111) in the Millibar Regime. *J. Phys. Chem. C* **2013**, *117* (32), 16438−16447.
(29) Trotochaud, L.; Head, A. R.; Karslıoğlu, O.; Kyhl, L.; Bluhm, H. Ambient Pressure Photoelectron Spectroscopy: Practical Considerations and Experimental Frontiers. *J. Phys.: Condens. Matter* **2017**, *29* (5), 053002.
(30) Jin, L.; Fu, Q.; Dong, A. Y.; Ning, Y. X.; Wang, Z. J.; Bluhm, H.; Bao, X. H. Surface Chemistry of CO on Ru(0001) under the Confinement of Graphene Cover. *J. Phys. Chem. C* **2014**, *118* (23), 12391−12398.
(31) Busse, C.; Lazić, P.; Djemour, R.; Coraux, J.; Gerber, T.; Atodiresei, N.; Caciuc, V.; Brako, R.; Blügel, S.; Zegenhagen, J.; et al. Graphene on Ir (111): Physisorption with Chemical Modulation. *Phys. Rev. Lett.* **2011**, *107* (3), No. 036101, DOI: 10.1103/PhysRevLett.107.036101.
(32) Gong, C.; Lee, G.; Shan, B.; Vogel, E. M.; Wallace, R. M.; Cho, K. First-Principles Study of Metal−Graphene Interfaces. *J. Appl. Phys.* **2010**, *108* (12), 123711.
(33) N'Diaye, A. T.; Coraux, J.; Plasa, T. N.; Busse, C.; Michely, T. Structure of Epitaxial Graphene on Ir(111). *New J. Phys.* **2008**, *10*, 043033.
(34) Balog, R.; Jorgensen, B.; Nilsson, L.; Andersen, M.; Rienks, E.; Bianchi, M.; Fanetti, M.; Laegsgaard, E.; Baraldi, A.; Lizzit, S.; Sljivancanin, Z.; Besenbacher, F.; Hammer, B.; Pedersen, T. G.; Hofmann, P.; Hornekaer, L. Bandgap Opening in Graphene Induced by Patterned Hydrogen Adsorption. *Nat. Mater.* **2010**, *9* (4), 315−319.
(35) Kyhl, L.; Balog, R.; Angot, T.; Hornekaer, L.; Bisson, R. Hydrogenated Graphene on Ir (111): A High-Resolution Electron Energy Loss Spectroscopy Study of the Vibrational Spectrum. *Phys. Rev. B: Condens. Matter Mater. Phys.* **2016**, *93* (11), 115403.
(36) Jørgensen, J. H.; Čabo, A. G. i.; Balog, R.; Kyhl, L.; Groves, M. N.; Cassidy, A. M.; Bruix, A.; Bianchi, M.; Dendzik, M.; Arman, M. A.; et al. Symmetry-Driven Band Gap Engineering in Hydrogen Functionalized Graphene. *ACS Nano* **2016**, *10*, 10798−10807.
(37) Balog, R.; Andersen, M.; Jorgensen, B.; Sljivancanin, Z.; Hammer, B.; Baraldi, A.; Larciprete, R.; Hofmann, P.; Hornekaer, L.; Lizzit, S. Controlling Hydrogenation of Graphene on Ir(111). *ACS Nano* **2013**, *7* (5), 3823−3832.
(38) Kyhl, L.; Bisson, R.; Balog, R.; Groves, M. N.; Kolsbjerg, E. L.; Cassidy, A. M.; Jørgensen, J. H.; Halkjær, S.; Miwa, J. A.; Čabo, A. G. Exciting H_2 Molecules for Graphene Functionalization. *ACS Nano* **2018**, *12*, 513.
(39) Hornekaer, L.; Sljivancanin, Z.; Xu, W.; Otero, R.; Rauls, E.; Stensgaard, I.; Laegsgaard, E.; Hammer, B.; Besenbacher, F. Metastable Structures and Recombination Pathways for Atomic Hydrogen on the Graphite (0001) Surface. *Phys. Rev. Lett.* **2006**, *96* (15), 156104.
(40) Pletikosic, I.; Kralj, M.; Pervan, P.; Brako, R.; Coraux, J.; N'Diaye, A. T.; Busse, C.; Michely, T. Dirac Cones and Minigaps for Graphene on Ir(111). *Phys. Rev. Lett.* **2009**, *102* (5). DOI: 10.1103/PhysRevLett.102.056808
(41) Lacovig, P.; Pozzo, M.; Alfe, D.; Vilmercati, P.; Baraldi, A.; Lizzit, S. Growth of Dome-Shaped Carbon Nanoislands on Ir (111): The Intermediate between Carbidic Clusters and Quasi-Free-Standing Graphene. *Phys. Rev. Lett.* **2009**, *103* (16), 166101.
(42) Doniach, S.; Sunjic, M. Many-Electron Singularity in X-Ray Photoemission and X-Ray Line Spectra from Metals. *J. Phys. C: Solid State Phys.* **1970**, *3* (2), 285.

DOI: 10.1021/acsanm.8b00610
ACS Appl. Nano Mater. 2018, 1, 4509−4515